PXIE END-TO-END SIMULATIONS*

J.-F. Ostiguy†, J.-P. Carneiro, V. Lebedev, A. Saini, N. Solyak
Fermilab, Batavia, IL 60540, USA

Abstract

Construction of PXIE, (Project-X Injector Experiment) has recently begun. The goal is to validate the design of the injector and low energy acceleration front-end for a future Project-X. PXIE operates in CW mode and consists in an ion source, a magnetically focused LEBT, a 162.5 MHz RFQ, a MEBT equipped with high bandwidth traveling wave kickers, a cryomodule equipped with 162.5 MHz half-wave resonators and a single cryomodule based on 325 MHz spoke resonators. The arrangement is meant to be closely representative of a future Project-X front end, and will include a variety of diagnostics. In this contribution we present end-to-end tracking simulations. We examine the impact of neutralization effects in the LEBT on the RFQ output emittances and losses within the MEBT and the superconducting cavities.

INTRODUCTION

The Project-X Injector Experiment (PXIE) aims at validating the design of the injector and low energy acceleration sections of a future Project-X. As such, its design closely follows the design of the Project-X front-end. A set of PXIE beam envelopes is shown in Fig. 1 with labels for the main sections. From left to right, PXIE starts with a 5 mA, 30 keV H^- source capable of delivering a maximum of 15 mA. Following the source, a low energy beam transport (LEBT) section ($\simeq$ 2 m long) delivers and matches the beam into an RFQ. Differential pumping is provided to prevent gas flow from the ion source to the RFQ. To reduce beam power during machine commissioning, the LEBT incorporates a pre-chopper capable of forming short beam current pulses (1-100 μs) at a 60 Hz rate. The RFQ is a four-vane, 4.4 m long device developed by LBNL operating in CW mode at a resonant frequency of 162.5 MHz. Its output energy of 2.1 MeV was chosen to lie below the neutron production threshold in copper.

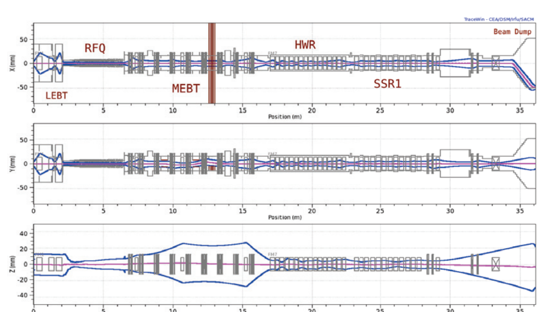

Figure 1: PXIE end-to-end 3σ beam envelopes. Top: (x, x'), Middle: (y, y'), Bottom: (z, z') . The MEBT is in shown operating in transmission mode. The beam sweep magnet is shown steering horizontally over the dump area.

The MEBT section is approximately 10 m long and matches optical functions between the RFQ and the input the of the first linac accelerating section (HWR). Optically, the MEBT consists of nine $\simeq 90°$ cells each comprising a quadrupole triplet and a dedicated purpose open section (65 cm). A key component of the MEBT is a high bandwidth bunch-by-bunch chopper to customize the bunch structure so as to satisfy experimental requirements. To reduce the required kick voltage, the chopper employs two (vertical) kickers separated by $180°$ in betatron phase. With one set of kick polarities the beam is transmitted after its centroid undergoes a small amplitude oscillation which is corrected downstream. With the reverse polarities, the triplets enhance the effect of the kickers, producing a higher amplitude oscillation which allows the beam to be completely intercepted by an absorber. The latter is designed to handle 21 kW of beam power, supporting operations with up to 10 mA beam current. Diagnostics to characterize the beam emerging from the RFQ are provided and are also integral to the machine protection system. Finally, differential pumping prevents potential performance degradation of the SRF cavities at the HWR cryomodule entrance.

Beam acceleration takes place within two SRF cryomodules (CMs), operating at $2°$ K and separated by a warm section. The the first cryomodule (designed and fabricated by ANL) consists in eight 162.5 MHz $\beta_g = 0.11$ half-wave resonators (HWR) separated by eight superconducting solenoids, each incorporating a pair of transverse corrector coils (H/V) and a BPM. The HWR cryomodule is 5.9 m long and takes the beam from 2.1 to 11 MeV. The second crymodule employs 325 MHz single-spoke resonators (SSR1) designed at FNAL. It consists of eight $\beta_g = 0.22$ resonators and 4 focusing solenoids. A corrector and BPM package is also integrated into each solenoid. The SSR1 cryomodule is 5.3 m long and accelerates the beam from 11 MeV to a final energy of 25 MeV. The beam properties and the beam extinction for rf buckets emptied by MEBT chopper are measured in a high-energy beam transport (HEBT) line. At the downstream extremity of the this line, PXIE terminates on a spectrometer magnet followed by a beam dump capable of dissipating 50 kW.

LEBT-RFQ MATCHING

The PXIE LEBT uses a 3-solenoid transport scheme (Fig. 2). The design incorporates two distinct regions. The first region is fully neutralized and extends from the exit

* US DOE contract DE-AC02-76CH03000
† ostiguy@fnal.gov

ISBN 978-3-95450-122-9

of the ion source assembly to a point located upstream of the chopper kicker, within the downstream fringe field region of solenoid no 2. The second region is un-neutralized and extends from the end of the neutralized region to the RFQ entrance. The rationale for this concept is to prevent neutralization transients from perturbing the optics during commissioning with a reduced duty-factor (effectively pulsed) beam. Should operation with an un-neutralized section prove unworkable, fully neutralized LEBT operation is also an option.

An RFQ captures incoming dc beam by adiabatically establishing transverse and longitudinal focusing. While the dc beam emerging from the source has a very small energy spread, the final longitudinal emittance of the bunches at the output depends directly on the energy spread introduced between the entrance and the end of the radial matching section, where longitudinal bunching is usually initiated. This spread arises because the off-axis electric field is nonzero; off-axis particles experience a small net acceleration or deceleration with respect to the on-axis synchronous particle.

For an ideal, regular transverse input distribution, one can determine the optimal input beam parameters $\bar{\alpha}$ and $\bar{\beta}$ that result in the smoothest possible transverse envelope. Generally these parameters result in minimal emittance growth and maximal transmission. Measurements performed on the ion source have shown that the emerging beam transverse phase space density is essential gaussian. Given the amount of free energy associated with a gaussian, simulations show – not surprisingly – that within an un-neutralized section some redistribution takes place i.e. the original phase space distribution spreads out. The effect is most noticeable through the third solenoid where the envelope needs to reach a high amplitude before rapidly decreasing in order to generate the convergence required at the RFQ entrance ($\alpha = \bar{\alpha}$) . A typical (3σ) beam envelope in the LEBT is shown in Fig. 2.

In terms minimizing losses, we find that attempting to match the rms parameters of the distribution does not necessarily lead to an optimal solution if space charge causes excessive emittance growth. One possible avenue is to reduce α at the RFQ input with respect to the matched value while keeping β matched. The effectiveness of this approach relies on the fact that the quality of the match into the RFQ tends to be more sensitive to beam size (β) than beam convergence (α). By allowing for a proportional reduction of amplitude in the last solenoid, a reduction in α also reduces emittance growth. Fig. 3 compares the distribution obtained at the output of a LEBT with an un-neutralized section with $\beta = \bar{\beta},\ \alpha = \frac{1}{2}\bar{\alpha}$ to that obtained at the output of a fully neutralized LEBT $\beta = \bar{\beta},\ \alpha = \bar{\alpha}$. Note the distinctive tails and the corresponding flattening of the projected spatial distribution with the un-neutralized section. Fig. 5 compares the emittance evolution through the RFQ obtained when propagating these distributions through the RFQ. For the un-neutralized LEBT case, there is a noticeable increase in transverse and longitudinal emittance.

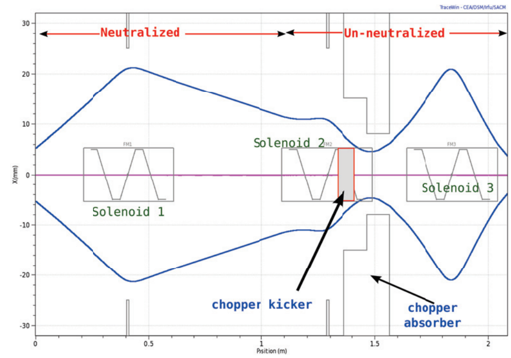

Figure 2: Beam envelope in the LEBT.

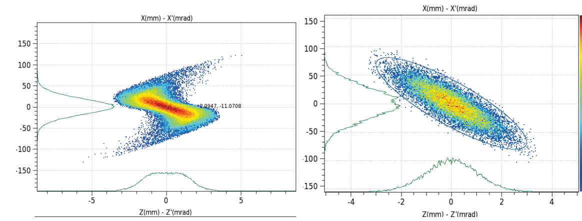

(a) Un-neutralized. $\alpha = \frac{1}{2}\bar{\alpha}$ (b) Neutralized, $\alpha = \bar{\alpha}$

Figure 3: Horizontal phase space at the RFQ input.

END-TO-END SIMULATIONS

As mentioned earlier, PXIE has two distinct optics each corresponding to a set of polarities of the high bandwidth kicker electrodes. With the transmission optics, a bunch is transmitted through the MEBT and subsequently accelerated in the HWR and SSR1 cryomodules to 25 MeV. Downstream of the SSR1 cryomodule, the beam goes through a deflecting cavity (no net kick is applied to a transmitted bunch) and finally reaches a 20 deg bend followed by a sweeping magnet to spread the beam over the dump area. With the extinction optics, a bunch is be deflected by the chopper onto the absorber located in the MEBT. Any residual beam is then steered by the deflecting cavity toward a sensitive particle detector, allowing an accurate measurement of achieved level of extinction. For the purpose of this paper, we concentrate on the transmission optics.

End-to end simulations were performed using the code TraceWin and its Toutatis RFQ module using 100k particles. Two cases were investigated. The first case assumes a partially neutralized LEBT tuned for $\alpha = \frac{1}{2}\bar{\alpha}$ at the RFQ input. The second assumes a fully neutralized LEBT but with the beam ideally matched at the same location.

Figs. 4 shows the beam particle density in the horizontal and vertical planes, from the MEBT input to the beam dump. Figs. 6 and 7 compare the predicted cumulative particle losses within the LEBT+RFQ and from the output of

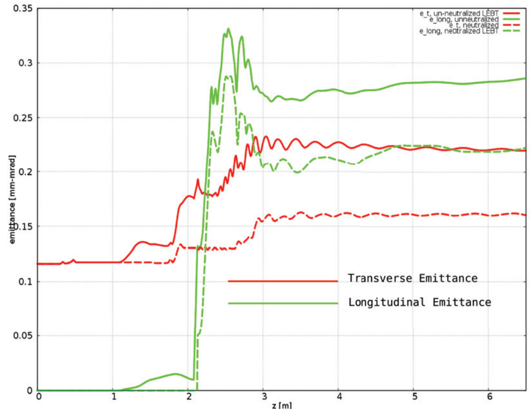

Figure 4: Emittance evolution through the RFQ. Solid: LEBT with un-neutralized section. Dashed: Fully neutralized LEBT.

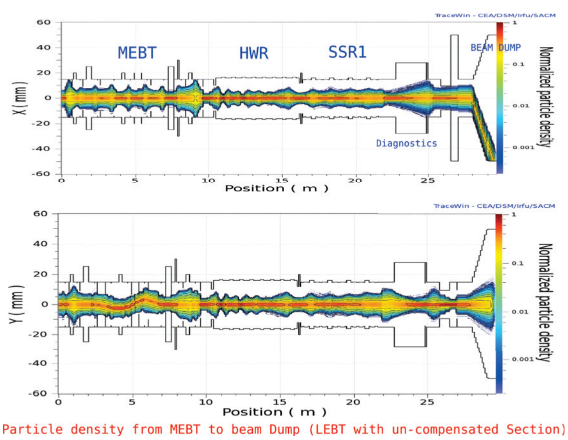

Figure 5: Particle density from the MEBT to the beam dump area.

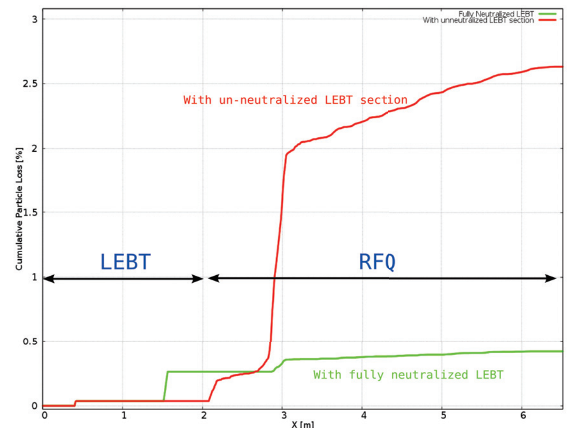

Figure 6: Cumulative particle losses from the source to the RFQ output.

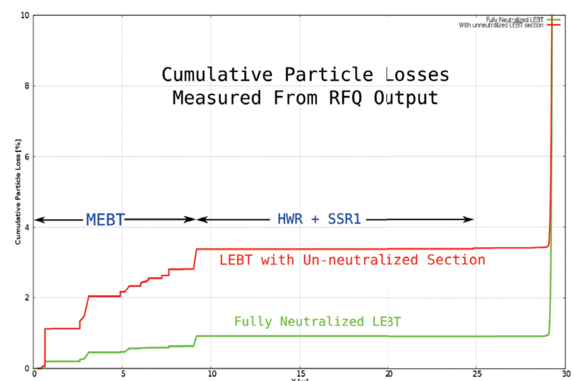

Figure 7: Cumulative particle losses from the MEBT to the beam dump.

the RFQ to the beam dump respectively. With the exception of solenoid 2 and 3 in the LEBT, the element settings are otherwise identical for both simulations. In both cases, no loss is observed in the superconducting cavities, which is the most critical region. However, operation with a non-compensated section would lead to a 2.5% loss in the RFQ and 3.5% loss in the MEBT. At full intensity, the beam power in the RFQ reaches a maximum of 1 kW at the output of the RFQ. A 2.5% loss therefore represents an upper bound of 250 W power loss to be dissipated, which is not a concern. In the MEBT, the higher emittances at the RFQ output associated with a LEBT operating with an un-neutralized section result in a 3.5% cumulative beam loss. This is technically less, than the 5% level specified as the tolerable limit for this section. Given the uncertainties associated with simulations, the design should be improved to provide a more comfortable margin in conjunction with a collimation strategy that does not necessarily avoid losses but rather ensures that the bulk of the losses are controlled losses. Adjustable collimators are planned at the input and output of the MEBT, downstream of the first quadrupole of the first and last sections. Note that while the input collimation sees a beam where all the buckets are occupied, the output collimator will see a beam where on average 80% of the buckets have been emptied by the broadband kicker.

CONCLUSION

The simulations reported here are an initial attempt at computing losses through PXIE. The results suggest that operation at full nominal power with a partially un-neutralized LEBT will require very careful optimization of the optics based on detailed simulations. An integral part of the process must be the optimization of the collimation strategy with the objective of ensuring that the bulk of the losses are controlled losses.

ACKNOWLEDGMENT

The authors would like to thank L. Prost and A. Shemyakin for discussions regarding the LEBT.

REFERENCES

[1] A. V. Shemyakin et al, "Project X Injector Experiment: Goals, Plan and Status", IPAC 13, Shanghai, TUOAB102

[2] S. Nagaitsev (Ed.) , "PXIE Design Handbook ", Fermilab, Jan 2013, `http://projectx-docdb.fnal.gov`

ISBN 978-3-95450-122-9